Noise Analysis of DMT

Georg Tauböck
Telecommunications Research Center Vienna (FTW)
Tech Gate Vienna, Donau-City-Strasse 1, A-1220 Vienna, Austria
phone: +43 1 505 2830-12 fax: +43 1 505 2830-99 email: tauboeck@ftw.at

***Abstract*— We consider Discrete Multitone (DMT, baseband OFDM) modulation and perform a detailed noise analysis which takes into account dependencies and power differences of real and imaginary part after the complex valued discrete Fourier transform (DFT). We show that for *colored* noise *rotated rectangular* symbol constellations are more appropriate than the common (quadratic) QAM symbol constellations with respect to capacity and symbol error probability, and we derive formulas for the rotation angles and constellation sizes/densities.**

I. Introduction

In this paper, we consider a Discrete Multitone (DMT) system as it is described for example in [1]. We mainly focus on the receiver part (see Fig. 1), especially on the noise characteristics disturbing the transmission.

First of all, observe that all operations in the receiver before the input of the decision device are linear operations. So it is sufficient to study the noise characteristics in the absence of a transmitted signal.

Throughout this paper, the noise at the input of the receiver is modeled as a discrete-time, real valued ($\Leftarrow$ **baseband**), wide-sense stationary (not necessarily Gaussian) random process $\mathbf{z} = [z(n)]_{n=-\infty,\ldots,+\infty}$, i.e., we are given the mean $\mu_{\mathbf{z}}(n) = \mathcal{E}\{z(n)\} = \mu_{\mathbf{z}}$ and the autocorrelation function[1] $R_{\mathbf{z}}(m+n, m) = \mathcal{E}\{z(m+n)z^*(m)\} = R_{\mathbf{z}}(n)$. Note that this model includes the practically more relevant assumption of **colored** noise[2].

In the following we analyze the first and second moments of the noise at the input of the frequency domain equalizer. From this we derive the moments at the input of the decision device.

The first part of the receiver transforms the random process at the input into a sequence of real random vectors. Each of these vectors has a first and second order description of its statistical properties, i.e., a mean vector and a covariance matrix. Due to the stationarity of the input random process all these mean vectors and covariance matrices are the same. Furthermore they do not depend on (time) shifts of the serial to parallel conversion. In the next part of the receiver each random vector of the sequence is passed through a discrete Fourier transform (DFT) which in turn produces a sequence of random vectors, this time complex valued. Note that for complex random vectors, mean vector and covariance matrix are not sufficient for a complete first and second order description of their statistical properties; one also needs the *pseudo-covariance* matrix[3]. The pseudo-covariance matrix $\mathbf{P_w} = [P_{\mathbf{w}}(k,l)]_{k,l=0,\ldots,N-1}$ of a complex random vector $\mathbf{w} = [w(k)]_{k=0,\ldots,N-1}$ is defined as $P_{\mathbf{w}}(k,l) = \mathcal{E}\{(w(k) - \mu_{\mathbf{w}}(k))(w(l) - \mu_{\mathbf{w}}(l))\}$, whereas the covariance matrix $\mathbf{C_w} = [C_{\mathbf{w}}(k,l)]_{k,l=0,\ldots,N-1}$ is defined as $C_{\mathbf{w}}(k,l) = \mathcal{E}\{(w(k) - \mu_{\mathbf{w}}(k))(w(l) - \mu_{\mathbf{w}}(l))^*\}$. Again, all mean vectors, covariance matrices, and pseudo-covariance matrices are the same and do not depend on previous (time) shifts of the serial to parallel conversion.

We proceed with the following definition.

Definition 1: A random vector is called *proper* (see [2]) or *rotationally invariant* (see [5]) or *circularly symmetric* (see [6]) if its pseudo-covariance matrix vanishes.

As it is shown in [2], for a proper random vector, real and imaginary part of an element of this random vector are uncorrelated and have identical variances. Using the theory of proper random vectors developed in [2] it can be easily seen that the random vectors at the output of the DFT are *not* proper except for the case when the input random vectors are constant with probability 1, i.e., - roughly speaking - they are deterministic[4]. This suggests that at the output of the DFT (and also at the input of the decision device) real and imaginary part at certain frequencies are correlated and/or have different variances in general.

Remark: In case of *passband* OFDM the situation is different. At the input of the receiver the demodulation of the signal (passband to baseband conversion) requires the calculation of an *analytical* signal. It is shown in [3] that the analytical signal of any stationary signal is proper. It follows that all considered random vectors are proper as well.

II. First and Second Moments

To verify this conjecture about correlations and variance differences, we calculate mean vector, covariance matrix and pseudo-covariance matrix of the complex random vector $\mathbf{w}_{n_0} = [w_{n_0}(k)]_{k=0,\ldots,N-1}$ at the output of the DFT (of even length $N \geq 2$) analytically. We assume (see Fig. 1) that the real (DFT-)input random vector $\mathbf{v}_{n_0} = [v_{n_0}(n)]_{n=0,\ldots,N-1}$ is part[5] of a discrete-time, real valued, wide-sense stationary random process $\mathbf{z} = [z(n)]_{n=-\infty,\ldots,+\infty}$ with mean $\mu_{\mathbf{z}}$ and

[1] The superscript * denotes complex conjugation, which is of course redundant for real valued random processes. Since we are dealing also with complex valued random processes later on, we write it here for completeness.

[2] Crosstalk is colored noise. The time domain equalizer transforms white noise into colored noise.

[3] or *complementary* covariance matrix (see [6])

[4] That is the only situation when a *real* random vector happens to be proper.

[5] Exactly this happens in the first block of the receiver (see Fig. 1).

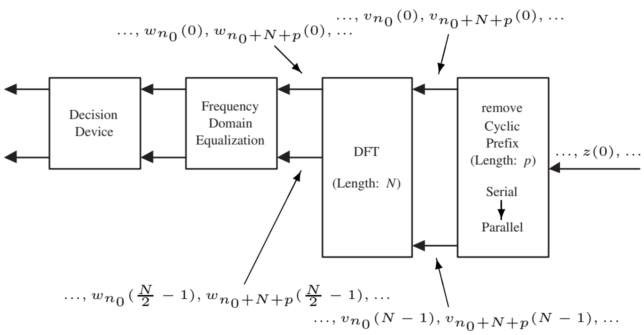

Fig. 1. Part of a DMT receiver

autocorrelation function $R_{\mathbf{z}}(n)$, i.e.,
$v_{n_0}(n) = z(n_0+n), \quad n = 0,\ldots,N-1$. We have

$$\begin{aligned} w_{n_0}(k) &= \frac{1}{\sqrt{N}}\sum_{n=0}^{N-1} v_{n_0}(n) e^{-j\frac{2\pi}{N}nk} \\ &= \frac{1}{\sqrt{N}}\sum_{n=0}^{N-1} z(n_0+n) e^{-j\frac{2\pi}{N}nk}, \\ k &= 0,\ldots,N-1, \quad \text{such that} \end{aligned} \tag{1}$$

$$\begin{aligned} \mu_{\mathbf{w}}(k) &= \mathcal{E}\{w_{n_0}(k)\} = \frac{1}{\sqrt{N}}\sum_{n=0}^{N-1}\mu_{\mathbf{z}} e^{-j\frac{2\pi}{N}nk} \\ &= \sqrt{N}\mu_{\mathbf{z}}\delta(k), \quad k=0,\ldots,N-1 \end{aligned} \tag{2}$$

with $\delta(0)=1$ and $\delta(k)=0$, $k \neq 0$.

Note that the mean vector $[\mu_{\mathbf{w}}(k)]_{k=0,\ldots,N-1}$ is real and does not depend on n_0.

With[6]

$$\begin{aligned} Q_{\mathbf{w}}(k,l) &= \\ &= \mathcal{E}\{w_{n_0}(k) w_{n_0}(l)\} \\ &= \tfrac{1}{N}\textstyle\sum_{n=0}^{N-1}\sum_{m=0}^{N-1}\mathcal{E}\{z(n_0+n)z(n_0+m)\} e^{-j\frac{2\pi}{N}(mk+nl)} \\ &= \tfrac{1}{N}\textstyle\sum_{n=0}^{N-1}\sum_{m=0}^{N-1} R_{\mathbf{z}}(n-m) e^{-j\frac{2\pi}{N}(mk+nl)} \end{aligned} \tag{3}$$

the elements of covariance and pseudo-covariance matrix of $\mathbf{w}_{n_0}$ can be written[7] as,

$$C_{\mathbf{w}}(k,l) = Q_{\mathbf{w}}(k,-l) - \mu_{\mathbf{w}}(k)\mu_{\mathbf{w}}(l), \tag{4}$$

$$P_{\mathbf{w}}(k,l) = Q_{\mathbf{w}}(k,l) - \mu_{\mathbf{w}}(k)\mu_{\mathbf{w}}(l). \tag{5}$$

The next step is to simplify the expression for $Q_{\mathbf{w}}(k,l)$. The idea is to reorder the terms of the double sum, such that only one sum remains (after some calculations). Here too, one defines $s = n-m$ and observes that $s \in \{-N+1,\ldots,N-1\}$. For the second required index $t \in \{0,\ldots,N-1-|s|\}$, we have to distinguish between the following cases:

$$\begin{aligned} s=0 &: \quad n=m=t \\ s>0 &: \quad n=s+t, \quad m=t \\ s<0 &: \quad m=|s|+t, \quad n=t. \end{aligned}$$

[6] $Q_{\mathbf{w}}(k,l)$ is also independent of n_0.
[7] Again no dependency on n_0.

This yields the following expression,

$$\begin{aligned} Q_{\mathbf{w}}(k,l) &= \frac{1}{N}R_{\mathbf{z}}(0)\sum_{t=0}^{N-1} e^{-j\frac{2\pi}{N}t(k+l)} + \\ &+ \frac{1}{N}\sum_{s=1}^{N-1} R_{\mathbf{z}}(s)\sum_{t=0}^{N-1-s}\Big(e^{-j\frac{2\pi}{N}(tk+sl+tl)} + \\ &\qquad + e^{-j\frac{2\pi}{N}(sk+tk+tl)}\Big). \end{aligned} \tag{6}$$

Using the formula

$$\sum_{t=0}^{M-1} a^t = \begin{cases} M, & a=1 \\ \frac{1-a^M}{1-a}, & a\neq 1 \end{cases}, \tag{7}$$

this further simplifies[8] to

$$Q_{\mathbf{w}}(k,l) = \tag{8}$$

$$= \begin{cases} R_{\mathbf{z}}(0) + 2\sum_{s=1}^{N-1} R_{\mathbf{z}}(s)\left(1-\frac{s}{N}\right)\cos\left(\frac{2\pi}{N}ks\right), \\ \qquad k+l=0 \text{ or } k+l=N \\ \underbrace{-\frac{\cot\left(\frac{2\pi}{2N}(k+l)\right)+j}{N}}_{-\frac{e^{j\frac{2\pi}{2N}(k+l)}}{N\sin\left(\frac{2\pi}{2N}(k+l)\right)}} \sum_{s=1}^{N-1} R_{\mathbf{z}}(s)\left(\sin\left(\frac{2\pi}{N}ks\right) + \right. \\ \qquad \left. + \sin\left(\frac{2\pi}{N}ls\right)\right), \\ \qquad k+l\neq 0 \text{ and } k+l \neq N \end{cases}.$$

III. Frequency Dependent Noise Analysis

Specializing the results of the previous section - see also [2] - one can calculate the covariance matrices (the frequency index $k = 1,\ldots,\frac{N}{2}-1$ is considered as a fixed parameter)

$$\mathbf{C}_{a,b}(k) = \begin{bmatrix} \sigma_a^2(k) & \gamma_{a,b}(k) \\ \gamma_{a,b}(k) & \sigma_b^2(k) \end{bmatrix}$$

of the real 2-dimensional random vectors $\begin{bmatrix} a_{n_0}(k) \\ b_{n_0}(k) \end{bmatrix}$, where $a_{n_0}(k) = \Re\{w_{n_0}(k)\}$ and $b_{n_0}(k) = \Im\{w_{n_0}(k)\}$, as

$$\begin{aligned} \sigma_a^2(k) &= \frac{R_{\mathbf{z}}(0)}{2} + \sum_{s=1}^{N-1} R_{\mathbf{z}}(s)\left(1-\frac{s}{N}\right)\cos\left(\frac{2\pi}{N}ks\right) - \\ &\quad - \frac{\cot\left(\frac{2\pi}{N}k\right)}{N}\sum_{s=1}^{N-1} R_{\mathbf{z}}(s)\sin\left(\frac{2\pi}{N}ks\right), \\ \sigma_b^2(k) &= \frac{R_{\mathbf{z}}(0)}{2} + \sum_{s=1}^{N-1} R_{\mathbf{z}}(s)\left(1-\frac{s}{N}\right)\cos\left(\frac{2\pi}{N}ks\right) + \\ &\quad + \frac{\cot\left(\frac{2\pi}{N}k\right)}{N}\sum_{s=1}^{N-1} R_{\mathbf{z}}(s)\sin\left(\frac{2\pi}{N}ks\right), \\ \gamma_{a,b}(k) &= -\frac{1}{N}\sum_{s=1}^{N-1} R_{\mathbf{z}}(s)\sin\left(\frac{2\pi}{N}ks\right). \end{aligned} \tag{9}$$

In general the noise variances (and thus the noise powers) for real and imaginary part are *different* and there are *statistical dependencies* between real and imaginary part.

[8] after a longer but straightforward calculation

Via eigenvalue decompositions, $\mathbf{C}_{a,b}(k)$ can be expanded into diagonal and orthonormal matrices $\mathbf{\Lambda}_{a,b}(k)$ and $\mathbf{U}_{a,b}(k)$, such that[9]

$$\mathbf{C}_{a,b}(k) = \mathbf{U}_{a,b}(k) \cdot \mathbf{\Lambda}_{a,b}(k) \cdot \mathbf{U}^{\mathbf{T}}_{a,b}(k). \tag{10}$$

Using (9), one calculates the diagonal eigenvalue matrices

$$\mathbf{\Lambda}_{a,b}(k) = \begin{bmatrix} \lambda_1(k) & 0 \\ 0 & \lambda_2(k) \end{bmatrix}$$

as

$$\begin{aligned} \lambda_1(k) &= \frac{R_{\mathbf{z}}(0)}{2} + \sum_{s=1}^{N-1} R_{\mathbf{z}}(s) \left(1 - \frac{s}{N}\right) \cos\left(\frac{2\pi}{N} ks\right) - \\ &\quad - \frac{1}{N \sin\left(\frac{2\pi}{N}k\right)} \sum_{s=1}^{N-1} R_{\mathbf{z}}(s) \sin\left(\frac{2\pi}{N} ks\right), \\ \lambda_2(k) &= \frac{R_{\mathbf{z}}(0)}{2} + \sum_{s=1}^{N-1} R_{\mathbf{z}}(s) \left(1 - \frac{s}{N}\right) \cos\left(\frac{2\pi}{N} ks\right) + \\ &\quad + \frac{1}{N \sin\left(\frac{2\pi}{N}k\right)} \sum_{s=1}^{N-1} R_{\mathbf{z}}(s) \sin\left(\frac{2\pi}{N} ks\right), \end{aligned} \tag{11}$$

and the orthonormal eigenvector matrices as

$$\mathbf{U}_{a,b}(k) = \begin{bmatrix} \cos\left(\frac{\pi}{N}k\right) & -\sin\left(\frac{\pi}{N}k\right) \\ \sin\left(\frac{\pi}{N}k\right) & \cos\left(\frac{\pi}{N}k\right) \end{bmatrix}. \tag{12}$$

It is important to observe that there are no correlations and variance differences between real and imaginary part at a certain frequency k if and only if $\lambda_1(k) = \lambda_2(k)$. Therefore it is natural to look at the difference $\lambda_2(k) - \lambda_1(k)$. From (11) we obtain

$$\begin{aligned} \lambda_2(k) - \lambda_1(k) &= \frac{2}{N \sin\left(\frac{2\pi}{N}k\right)} \sum_{s=1}^{N-1} R_{\mathbf{z}}(s) \sin\left(\frac{2\pi}{N} ks\right) \\ &= \frac{2}{N \sin\left(\frac{2\pi}{N}k\right)} \Im \left\{ \sum_{s=1}^{N-1} R_{\mathbf{z}}(s) e^{j\frac{2\pi}{N}ks} \right\} \end{aligned} \tag{13}$$

and using the properties of the DFT/IDFT (see for example [7]) we are now able to state the following theorem.

Theorem 1: Correlations and variance differences between real and imaginary part of the noise at the output of the DFT do *not* occur at *any* frequency $k = 1, \ldots, \frac{N}{2} - 1$ if and only if the autocorrelation function $R_{\mathbf{z}}(n)$ satisfies the relation $R_{\mathbf{z}}(n) = R_{\mathbf{z}}(N - n)$ for $n = 1, \ldots, N - 1$.

Note that the same theorem holds essentially for the noise at the input of the decision device, because the frequency domain equalizer performs simple multiplications with complex numbers for each frequency, which corresponds to rotations (phase) and scalings (absolute value) in the complex plane (for each frequency separately).

[9] $\mathbf{U}^{\mathbf{T}}_{a,b}(k)$ denotes the transposed matrix $\mathbf{U}_{a,b}(k)$

Remarks: Theorem 1 tells us that correlations and/or variance differences occur only in the presence of **colored** noise. It is obvious that in practical systems the condition of Theorem 1 on the autocorrelation function is never fulfilled. So one has to be aware that the noise powers for real and imaginary part are different.

IV. Consequences and Asymptotic Analysis

Consider again a common DMT system as described in [1]. In the transmitter the bit stream is mapped onto QAM-symbols of size and density which depend on the noise power of the corresponding carrier/frequency, e.g., according to the water filling solution. But this implicitly assumes that the noise power of real and imaginary part are equal. As we showed in the previous sections this is not the case in general. To overcome this problem one has to use *rotated rectangular* complex symbol alphabets. The angles of the rotations are given by the orthonormal eigenvector matrices[10], c.f. (12), whereas size and density are determined by the eigenvalues, c.f. (11).

Theorem 2: The rotation angles $\phi(k) = \frac{\pi}{N}k$, $k = 1, \ldots, \frac{N}{2} - 1$ are *independent* of the mean $\mu_{\mathbf{z}}$ and the autocorrelation function $R_{\mathbf{z}}(n)$ of the noise at the input of the receiver.

To get a better picture of the deviations of the (ideal) rotated rectangular constellations from the common QAM constellations, we have to look at the relative differences

$$d(k) = \frac{\lambda_2(k) - \lambda_1(k)}{\lambda_1(k) + \lambda_2(k)} = \frac{\lambda_2(k) - \lambda_1(k)}{\sigma_a^2(k) + \sigma_b^2(k)}. \tag{14}$$

We omit an analytic treatment of the relative differences. Instead we first provide some simulation results, and then analyze (analytically) what happens if N goes to infinity for a special choice of $R_{\mathbf{z}}(n)$.

A. Simulation Results

From Fig. 2 one can see that significant differences between ideal rectangular constellations and the used QAM constellations may occur. The noise is zero mean filtered white Gaussian noise with filter impulse response (q is a fixed parameter)

$$g_q(n) = \begin{cases} \left(1 - \cos\frac{2\pi n}{N}\right) \cos\frac{2\pi q n}{N}, & n = 0, \ldots, N-1 \\ 0, & n \neq 0, \ldots, N-1 \end{cases}. \tag{15}$$

Note that 1 is the maximum value $|d(k)|$ can take (in this case: $\lambda_1(k) = 0$ or $\lambda_2(k) = 0$).

B. Asymptotic Analysis

In the following we assume that the random noise process at the input of the receiver is zero mean and has an autocorrelation function

$$R_{\mathbf{z}}(n) = \begin{cases} 1, & n = 0 \\ \frac{1}{2}, & n = -1 \text{ or } n = 1 \\ 0, & n \neq -1 \text{ and } n \neq 0 \text{ and } n \neq 1 \end{cases}. \tag{16}$$

[10] These matrices are rotation matrices

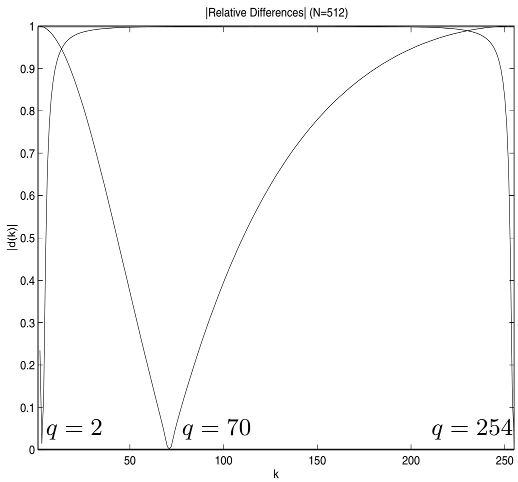

Fig. 2. Relative differences. The noise is zero mean filtered white Gaussian noise with variance 1.

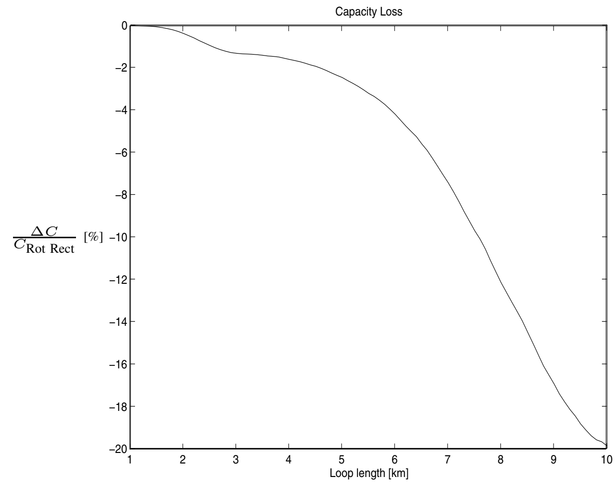

Fig. 3. Normalized capacity loss in terms of loop length.

The corresponding relative (eigenvalue) difference at frequency $\frac{N}{2} - 1$ is given by

$$d(\frac{N}{2} - 1) = \frac{1}{N - (N-1)\cos\left(\frac{2\pi}{N}\right)}, \tag{17}$$

which tends to 1 if N tends to infinity. This shows that in general an increasing DFT-length N does *not* decrease this effect. On the contrary, there are frequencies (depending on N) for which rectangular symbol constellations become more and more appropriate.

V. Capacity Loss

In order to use rotated rectangular constellations one has to modify the existing bit-loading/mapping algorithms, such that they take into account the powers of the real and imaginary parts of the noise. Note that the rotation angles do not depend on the actual noise characteristics (see Theorem 2) and need not be estimated during transmission. On the other hand if one sticks to the conventional QAM constellations one has to accept significantly enhanced symbol error probability (at least if there is no appropriate coding, c.f. Sec. VI) and decreased capacity. Specializing the results of [4] one obtains the following (approximate) expression[11] for the capacity loss [bits / channel use],

$$\begin{aligned} \Delta C &= C_{\text{QAM}} - C_{\text{Rot Rect}} \approx \\ &\approx \frac{1}{2(N+p)} \sum_{k=1}^{\frac{N}{2}-1} \log_2 \left(1 - \frac{(\lambda_1(k) - \lambda_2(k))^2}{L^2 \left| H\left(e^{\frac{j2\pi k}{N}}\right)\right|^4} \right), \end{aligned} \tag{18}$$

where $H(z)$ denotes the channel transfer function, and p and L are the length of the cyclic prefix[12] and the water level (*Water Filling*), respectively. Note that L depends on the signal power.

[11] Valid for Gaussian distributed noise

[12] The division by $N + p$ originates from the serial-to-parallel conversion, the conjugate complex extension and the addition of the cyclic prefix.

We performed some simulations in order to demonstrate the capacity loss. We used the parameters of a real *ADSL* scenario, i.e., a DFT-length of 512, a subcarrier spacing of 4312.5 Hz, and a transmit power of 100 mW. The transfer functions of the loops were obtained by measurements of Austrian cables. The noise model was as follows: we assumed two additive, statistically independent noise components. One was the typical noise environment in a cable bundle including crosstalk and background noise. The other was stationary narrowband interference with a bandwidth of 10 kHz, center frequency of 1.07 MHz, and 0 dBm power. The normalized capacity loss depending on the loop length can be seen in Fig. 3.

VI. Symbol Error Probability and Optimized Bit-Loading

Let's assume that a certain conventional bit-loading algorithm assigns to the k-th subcarrier a QAM constellation consisting of signal points,

$$\left\{ \begin{array}{c} t_1 V_1(k) + j t_2 V_2(k) : \\ t_1 \in \{\pm 1, \pm 3, \ldots, \pm (M_1(k) - 1)\} \\ t_2 \in \{\pm 1, \pm 3, \ldots, \pm (M_2(k) - 1)\} \end{array} \right\}, \tag{19}$$

where $V(k) = V_1(k) = V_2(k)$ is a certain gain factor and $M(k) = M_1(k) = M_2(k)$ is the number of signal points in real and imaginary part direction, respectively. Note that the whole number of signal points is $M_{\text{all}}(k) = (M(k))^2$. If these signal points are chosen with equal probabilities during transmission, the average signal power is calculated as

$$S_{\text{all}}(k) = \frac{2}{3} (V(k))^2 (M_{\text{all}}(k) - 1) \approx \frac{2}{3} (V(k))^2 M_{\text{all}}(k), \tag{20}$$

the approximation being good, provided that the number of signal points $M_{\text{all}}(k)$ is not too small. At the input of the decision device, the eigenvalues of the covariance matrices of real and imaginary parts of the noise at certain frequencies are given by (see also [1])

$$\mu_1(k) = \left|H\left(e^{\frac{j2\pi k}{N}}\right)\right|^{-2}\lambda_1(k), \qquad (21)$$
$$\mu_2(k) = \left|H\left(e^{\frac{j2\pi k}{N}}\right)\right|^{-2}\lambda_2(k).$$

In the following we will assume $\mu_1(k) > \mu_2(k)$ without loss of generality. In the presence of Gaussian noise the symbol error probabilities can be approximated by[13]

$$P_{\text{QAM}}(k) \approx 2Q\left(\sqrt{c\cdot\frac{3S_{\text{all}}(k)}{2M_{\text{all}}\mu_1(k)}}\right), \qquad (22)$$

where $c = 1$ is an approximation, which neglects the noise rotations (but not the power differences), and $c = 2$ and $c = \frac{1}{2}$ yield lower and upper bounds, respectively, which are valid for all possible rotation angles. Note that the noise rotations at the input of the decision device are not only determined by Theorem 2, they also depend on $\arg\left(H\left(e^{\frac{j2\pi k}{N}}\right)\right)$.

By straightforward optimization (with respect to symbol error probability) it can be shown (analytically) that a bit-loading algorithm which takes into account power differences and statistical dependencies between real and imaginary parts of the noise distributes the same signal power onto the two axes of the rotated rectangular constellations, $S_1(k) = S_2(k) = \frac{S_{\text{all}}(k)}{2}$. Furthermore, the optimum numbers of signal points into the two directions are derived as

$$M_1(k) = \sqrt{M_{\text{all}}(k)}\left(\frac{\lambda_2(k)}{\lambda_1(k)}\right)^{\frac{1}{4}}, \qquad (23)$$
$$M_2(k) = \sqrt{M_{\text{all}}(k)}\left(\frac{\lambda_1(k)}{\lambda_2(k)}\right)^{\frac{1}{4}},$$

which, of course, have to be rounded to even numbers. Observe the optimization constraints $S_1(k) + S_2(k) = S_{\text{all}}(k)$ and $M_1(k)M_2(k) = M_{\text{all}}(k)$. Via

$$S_i(k) = \frac{1}{3}\left(V_i(k)\right)^2\left(\left(M_i(k)\right)^2 - 1\right), \quad i = 1, 2, \qquad (24)$$

the gain factors $V_i(k)$, c.f. (19), are determined as well. The symbol error probabilities are calculated as

$$P_{\text{Rot Rect}}(k) \approx 4Q\left(\sqrt{\frac{3S_{\text{all}}(k)}{2M_{\text{all}}\sqrt{\mu_1(k)\mu_2(k)}}}\right), \quad \text{such that} \qquad (25)$$

we obtain (approximate) SNR[14] gains

$$G(k) = \frac{\text{SNR}_{\text{Rot Rect}}(k)}{\text{SNR}_{\text{QAM}}(k)} \approx \frac{1}{c}\sqrt{\frac{\mu_1(k)}{\mu_2(k)}} = \frac{1}{c}\sqrt{\frac{\lambda_1(k)}{\lambda_2(k)}}, \qquad (26)$$

where c has the same meaning as in equation (22). Finally, we can express the gains in terms of the relative (eigenvalue) differences as

$$G(k) \approx \frac{1}{c}\sqrt{\frac{1 + |d(k)|}{1 - |d(k)|}}. \qquad (27)$$

[13]The Q-function is defined as $Q(x) = \frac{1}{2\pi}\int_x^\infty e^{-\frac{t^2}{2}}\,dt$.

[14]The SNR is defined via $P \sim Q\left(\sqrt{\text{SNR}}\right)$

We want to emphasize that in our previous examples (see Fig. 2 and Sec. V) the modulus of the relative differences is close to 1 for almost all frequencies, such that the overall SNR gain is very dramatic, no matter of the value of c.

Remarks: The SNR gains are independent of the channel transfer function and of the signal power and thus of the loop length, which is not the case for the capacity loss. Furthermore, the previous examples show that the use of rotated rectangular constellations is much more effective in reducing the (uncoded) symbol error probability than in increasing capacity. Note that statements about capacity always assume an optimum coding strategy which is not applicable in practice. For practical en-/decoders the overall gain will be somewhere in between. It depends on the ability of the code to use the safer transmission in one direction (corresponding to one eigenvector) to correct the more frequent errors in the other direction (corresponding to the other eigenvector). The effort required to adapt the coding strategy is much higher than for implementing rotated rectangular constellations.

VII. Conclusions

We considered a DMT transmission system and analyzed the noise after the DFT and at the input of the decision device. With an analytical approach we were able to show that there are dependencies and/or power differences between the real and imaginary part of the noise at certain frequencies and to derive formulas for the corresponding 2-dimensional covariance matrices, its eigenvalues, and eigenvectors. We presented a simple criterion for the occurrence of dependencies and/or power differences which only requires the knowledge of the autocorrelation function of the random noise process at the input of the receiver. We examined these formulas and emphasized that **rotated rectangular symbol constellations** are much better than the common QAM constellations with respect to capacity and symbol error probability. The rotation angles are *independent* of the actual noise characteristics and need not be estimated during transmission. We presented an optimized bit-loading algorithm which produces dramatic gains in terms of symbol error probability. Finally, we provided some simulation plots, which confirmed the theoretical results and demonstrated the relevance of this work.

References

[1] R. Fischer, *Mehrkanal- und Mehrträgerverfahren für die schnelle digitale Übertragung im Ortsanschlussleitungsnetz*, PhD thesis. Universität Erlangen/Nürnberg, Germany, 1996.

[2] F. D. Neeser, *Communication Theory and Coding for Channels with Intersymbol Interference*, PhD thesis. ETH Zürich, Switzerland, 1993.

[3] B. Picinbono, *Random Signals and Systems*. Englewood Cliffs, NJ: Prentice-Hall, 1993.

[4] G. Tauböck, "Rotationally Variant Complex Channels," in *Proc. 23rd Symposium on Information Theory in the Benelux*, Louvain-la-Neuve, Belgium, May 29-31, 2002.

[5] A. Lampe, R. Schober, and W. H. Gerstacker, "Iterative Multiuser Detection for Complex Modulation Schemes," in *Proc. IEEE International Symposium on Information Theory (ISIT)*, Washington D.C., p. 33, 2001.

[6] E. A. Lee, and D. G. Messerschmitt, *Digital Communication*, 2nd ed. Boston/Dordrecht/London: Kluwer Academic Publishers, 1994.

[7] A. W. M. Van Den Enden, and N. A. M. Verhoeckx, *Discrete-Time Signal Processing, An Introduction*. Prentice Hall, 1989.

